Following Potential Vorticity and Pollution across the Pacific – Spring 2001
Part I: Mainly Layers in Pollution

Reginald E. Newell and Yuanlong Hu
Department of Earth, Atmospheric and Planetary Sciences,
Massachusetts Institute of Technology, Cambridge, MA

Valérie Thouret
Laboratoire d'Aérologie, Université-Paul Sabatier, Toulouse, France

Edward V. Browell, Marta A. Fenn, and David J. Westberg
NASA, Langley Research Center, Hampton, VA

Abstract.

We have summarized the properties of layers measured during NASA's Transport and Chemical Evolution Over the Pacific Experiment (TRACE-P) carried out between February and April 2001, for layers that involve water vapor, ozone, carbon monoxide, and methane. There were 466 layers, with an average thickness of 0.56 kilometers, an average altitude of 5.3 kilometers, and they occupied about 21% of the total atmosphere. When water vapor was low and ozone high, there were about 70 cases when carbon monoxide and methane were low, suggesting that these were stratospheric layers. A significant fraction of other stratospheric layers could also have been involved with collisions. A second paper is in preparation involving a broader description of potential vorticity.

1. Introduction

We have studied the distribution of potential vorticity and pollution, especially ozone, in their motions across the Pacific during NASA's Transport and Chemical Evolution Over the Pacific Experiment (TRACE-P) carried out between February and April 2001. The description of the experiment has been presented by Jacob et al. (*this issue*) and the meteorological conditions by Fuelberg et al. (*this issue*). Our main interest has been in the occurrence of potential vorticity and pollution, particularly ozone, and there interactions, particularly in the form of layers within the atmosphere. Rather than reciting these findings directly (e.g. Newell et al., 1999), we have tried to summarize them indirectly. The two aircraft used, the P-3B and the DC-8, have certain planned tasks set out roughly before the experiment and these were followed fairly closely. The fraction of the atmosphere explored was, in a sense, determined before the start of the mission. We would like to know, where, in this fraction were PV or O_3 found and how were they related. In the previous studies we found that layers occupied up to 20% of the troposphere, their mean thickness was between 0.6-0.8 km, and their average altitude was about 6 km; overall, a sample of over 22,000 layers were examined. We plan to extend the coverage slightly during this paper, then move towards an expansion of the parameters by including additional information such as potential vorticity.

2. Background Information

The layers were classified, as carried out previously by Stoller et al. (1999), Newell et al. (1999), and Thouret et al. (2000, 2001). Layers in the vertical profiles made by the aircraft were identified from deviations exceeding specified thresholds from averaged background concentrations. These thresholds are set to ±10 ppbv for ozone; ±5% for relative humidity; ±3 ppbv for carbon monoxide and methane. Water vapor and ozone were divided into four groups with anomalies processed from their averages (as seen in Table 1). They are exhibited geographically in Plate 1; clearly there is an abundance of layers in routes leading out of Hong Kong. The layers are colored according to their average altitude as noted. As before the main contribution comes from species that have high ozone and low water vapor (254 out of 466 layers, see Plate 2). The other three types are about equally distributed. If we expand the type 2 (high ozone and low water vapor) to include methane and carbon monoxide, then the high ozone, low water vapor, carbon monoxide and methane gives over 70 cases, while the high ozone, low water vapor, high carbon monoxide and high methane also give almost 70 cases. The former came directly from a stratospheric source and the latter could have been involved in a collision between layers with the stratospheric layer colliding from the top with the pollution layer (Cho et al., 2001). This provides a separate way of using the layer distributions. Finally the layer thicknesses versus height do not show much variability.

3. Subdivision of Layers

Type 1 (Plate 3a) has ΔO_3 and ΔH_2O positive with the CO and CH_4 anomalies distributed among their four possibilities. The largest number, with 22 cases, was to see four types all with four positive anomalies. Five of these were found above 8 km, and could well have originated in the boundary layer.

Type 2A is a layer with (locally) O_3 high, H_2O low, and both CO and CH_4 high (Plate 3b). This could be a layer that has emerged from the stratosphere to the troposphere and then been superposed by downwards transit to continue with a polluted tropospheric layer. Type 2B could be a similar circumstance with a negative CH_4 anomaly; while Type 2C could be a similar circumstance with a negative CO anomaly. Type 2D would be a clear cut stratospheric feature with both CO and CH_4 being diminished within the stratosphere. Out of this set then, three out of four types would be involved with layer collisions; only 2D would be a clear-cut stratospheric layer.

Type 3 has an O_3 anomaly which is negative and an H_2O anomaly which is positive (Plate 3c), the largest value having both ΔCO and ΔCH_4 negative and the second largest having these two anomalies positive. One could speculate that the first combination denotes material that started in the boundary layer over the ocean, where O_3 anomaly is often negative. Three negatives, ΔO_3, ΔCO and ΔCH_4, could represent relatively clean air. Two positives, ΔCO and ΔCH_4, could represent polluted air.

Type 4 has both ΔO_3 and ΔH_2O values negative with the largest of the sub-categories having ΔCO and ΔCH_4 also negative (Plate 3d). This could be indicated to show a lack of pollution in an air mass that had spent some time in the upper troposphere away from sources. Positive methane or carbon monoxide deviation could indicate possible contamination with pollution. This completes the overview of four sets of anomalies with the four variables. Overall, and as before, the main finding stands – that the coupled ΔO_3 positive and ΔH_2O negative give the largest contribution to the organization of the layers.

The data collected in Figure 3, following the combination of four traces H_2O, O_3, CO, and CH_4, are summarized in Table 1. This resembles the table used by Stoller et al. (1999). Layers 2A and 2D have the maximum number of observations about 70, out of the 315 total. A number of these layers have been involved in coupling, as we said previously. Probably only the rich O_3 and poor H_2O, CO and CH_4 layers came directly from the stratosphere.

The previous data, coupled with TRACE-P, are summarized in Table 2. MOZAIC data are still the main set of data but it is clear that the processes occurring elsewhere follow the trend of MOZAIC. Out of a total of 105, 498 km profiles, 22,380 layers were sampled for a net coverage of 17%. This data is updated from a paper by Newell et al. (1999).

4. Reconstruction following ozone, water and other tracers

In the few examples given here we start with the ozone record, then move forward to other tracers. Where appropriate we will also include potential vorticity. Its use will be expanded in the second paper. The first case selected was DC-8, Flight 5 for 27 February 2001, from Kona, Hawaii to Guam. There was an extensive layer about 3800 km long, from about 162˚W to 162˚E, Plate 4; with ozone about 70 ppbv, CO was about 230 ppbv and the layer was dry. The track is shown geographically at about 305K (~800 hPa) in Plate 5. Following the prescription under section 3 this layer was originally part of a collision in the troposphere with an upper level stratospheric layer impacting a polluted layer. The other pollutants in the layer, for example, HNO_3 (399 pptv maximum) and butane (39 pptv maximum) were not especially high so did not fall into a characteristic maximum tendency. Even the propane/ethane ratios were low (0.31 cp a maximum of 0.9) indicating fairly old data. The water vapor layer showed enhanced cooling near its base (~2 km up to 7˚C per day, Figure 1); the cooling dropped to almost zero near the top of the layer. This radiative tendency produced stabilization. The fact that the layer was steady at the same altitude for most of its life was another indicator of stability.

Jim Hoell (personal communication) found similar evidence of a collision from studies he undertook with the trajectories from Florida State University. Our high potential vorticity (~5 x 10^{-7} K m^2/kg/s) appears near the base of the ozone layer, producing an internal consistency between the lidar ozone, the trajectories and the other trace constituents.

On March 4, 2001 both planes flew from Guam to Hong Kong, starting with parallel tracks at 2000 feet. After the separation at about 0430UT the DC-8 intercepted high pollution at about 1000 feet, 27˚N, 125˚E (propane/ethane at about 0.4 and ozone reaching about 120 ppbv). At a later time (0700UT) the highest carbon monoxide was 380 ppbv measured by the DC-8 accompanied by a battery of other high level pollutants (but not ozone). At the same time the P3-B encountered very poor visibility and high values of pollutants with CO about 400 ppbv and many other pollutants amplified (except ozone).

One of the largest plumes seen from TRACE-P was the Shanghai plume, reported by several investigators including Jacob et al. (this issue), Singh et al. (this issue), Kiley et al. (this issue), Talbot et al. (this issue), and Simpson et al. (this issue). The latter two papers each devotes a considerable portion to this plume. There is evidence of high potential vorticity (>85 x 10^{-7} K m^2/kg/sec) suggesting, even though most of the plume had a lower level source, that some material originated from high levels (Plates 6 and 7). As pointed out by Kiley et al. (this issue), simulated CO from various chemical transport models for flight 13 is greatly underestimated and is among the worst when compared to that of other missions. Incidentally, the ozone sampled in the stratosphere was 388 ppbv, nearly the highest on the mission. The propane/ethane ratio was 4/192, one of the lowest on the mission, demonstrating the lack of non-methane hydrocarbons in this portion of the stratosphere. Higher ozone was reported for Mission 20D (700 ppbv) and Mission 17D (550 ppbv). In Mission 20D ozone was 697 ppbv with carbon monoxide only 17 ppbv (propane was in the noise). In Mission 17 ozone was 426 ppbv and the propane/ethane ratio was 7/147, again denoting a lack of non-methane hydrocarbons, with carbon monoxide down to 28 ppbv. These ozone values all seemed to originate from the stratosphere.

5. Conclusion

As for earlier missions we have taken a census of atmospheric layers involving ozone, water vapor, carbon monoxide, and methane. We compared their occurrence with similar layers in previous missions. The dimensions, including thickness, were quite similar, as was the abundance property; they are matched in Table 2. Thickness of 0.56 kilometers, heights ranging from 4.9 to 5.8 kilometers, and all together occupying about 21% of the atmosphere. These dimensions are similar to those found earlier. The predominance of the layers from the stratosphere gives an important role to their major place in sharing space between the troposphere and the stratosphere. While this analysis has centered on the pollution aspects, of equal importance is the role of potential vorticity in the dynamic role relating troposphere and stratosphere. This topic will be investigated in a separate paper.

Acknowledgment. The MIT contribution to this paper came from NASA grant NCC-1-415.

References

Browell, E. V., and 22 others, Large-scale air mass characteristics observed over the remote tropical Pacific Ocean during March-April 1999: Results from PEM-Tropics B field experiment, *J. Geophys. Res., 106*, D23, 32,481-32,502, 2001.

Cho, J. Y. N., R. E. Newell, B. E. Anderson, J. D. W. Barrick, and K. Lee Thornhill, Characterizations of tropospheric turbulence and stability layers from aircraft observations, *J. Geophys. Res*., TRACE-P Special Section, (submitted).

Fuelberg, H. E., C. M. Kiley, J. R. Hannan, D. J. Westberg, M. A. Avery, and R. E. Newell, Atmospheric transport during the transport and chemical evolution over the Pacific (TRACE-P) experiment, *J. Geophys. Res*., TRACE-P Special Section, (submitted).

Jacob, D. J., J. H. Crawford, M. M. Kleb, V. E. Connors, R. J. Bendura, and J. L. Raper, The transport and chemical evolution over the Pacific (TRACE-P) mission: design, execution, and overview of results, *J. Geophys. Res*., TRACE-P Special Section, (submitted).

Kiley, C. M., H. E. Fuelberg, D. Allen, G. R. Carmichael, D. J. Jacob, C. Mari, P. I. Palmer, B. Pierce, K. Pickering, Y. Tang, O. Wild, T. D. Fairlie, J. A. Logan, D. G. Streets, An intercomparison and validation of aircraft-derived and simulated CO from seven chemical transport models during the TRACE-P experiment, *J. Geophys. Res*., TRACE-P Special Section, (submitted).

Newell, R. E., V. Thouret, J. Y. N. Cho, P. Stoller, A. Marenco, and H. G. Smit, Ubiquity of quasi-horizontal layers in the troposphere, *Nature, 398*, 316-319, 1999.

Simpson, I., N. Blake, E. Atlas, F. Flocke, J. Crawford, H. Fuelberg, C.M. Kiley, F. S. Rowland, and D. Blake, Photochemical production and evolution of selected C2-C5 alkyl nitrates in tropospheric air influenced by Asian outflow, *J. Geophys. Res*., TRACE-P Special Section, (submitted).

Singh, H. B., L. Salas, D. Herlth, E. Czech, W. Viezee, Q. Li, D. J. Jacob, D. Blake, G. Sachse, C. N. Harward, H. Fuelberg, C. M. Kiley, In-situ measurements of HCN and CH3CN in the Pacific troposphere: sources, sinks, and comparisons with spectroscopic observations, *J. Geophys. Res*., TRACE-P Special Section, (submitted).

Stoller, P., J.Y.N. Cho, R.E. Newell, V. Thouret, Y. Zhu, M.A. Carroll, G.M. Albercook, B.E. Anderson, J.D.W. Barrick, E.V. Browell, G.L. Gregory, G.W. Sachse, S. Vay, J.D. Bradshaw and S. Sandholm, Measurements of atmospheric layers from the NASA DC-8 and P-3B aircraft during PEM-Tropics A, *J. Geophys. Res*., *104*, D5, 5745-5764, 1999.

Talbot, R., J. Dibb, E. Scheuer, G. Seid, R. Russo, S. Sandholm, D. Tan, H. Singh, D. Blake, N. Blake, E. Atlas, G. Sachse and M. Avery, Reactive nitrogen in Asian continental outflow over the Western Pacific: Results from the NASA TRACE-P airborne mission, *J. Geophys. Res*., TRACE-P Special Section, (submitted).

Thouret, V., J. Y. N. Cho, R. E. Newell, A. Marenco, and H. G. J. Smit, General characteristics of tropospheric trace constituent layers observed in the MOZAIC program, *J. Geophys. Res.*, 105, 17,379-17,392, 2000.

Thouret, V., J. Y. N. Cho, M. J. Evans, R. E. Newell, M. A. Avery, J. D. W. Barrick, G. W. Sachse, and G. L. Gregory, Tropospheric ozone layers observed during PEM-Tropics B, *J. Geophys. Res.*, 106, 32,527-32,538, 2001.

Figure 1. Vertical profiles of O_3, CO, air/dew-point temperatures, and H_2O heating rate sampled during TRACE-P DC-8 mission 5 around 22:40 UTC, February 27, 2001, near 18ºN, 175ºW.

Plate 1. Geographical distribution of layers based on ozone and water vapor. Symbols indicate layers with rich O_3 and H_2O (triangles); rich O_3 and poor H_2O (circles); poor O_3 and rich H_2O (diamonds); poor O_3 and H_2O (squares). Layers are colored according to their altitudes fallen into 1 km bins shown in the color bar.

Plate 2. Same as Figure 1 with each category (based O_3 and H_2O only) displayed separately. Number of observations is indicated on each panel.

Plate 3. Geographical distribution of layers based on O_3, H_2O, CO, and CH_4 for (a) Type 1; (b) Type 2; (c) Type 3; (d) Type 4. Number of observations is indicated on each panel.

Plate 4. Along track cross-section of LIDAR O_3 (color shaded, in ppbv) and potential vorticity (contours, in 10^{-7} K m^2 kg^{-1} s^{-1}) for TRACE-P DC-8 flight 5 (Kona to Guam). Flight track is indicated by the red line.

Plate 5. Potential Vorticity (shaded, in 10^{-7} K m^2 kg^{-1} s^{-1}), pressure (green contours, in hPa), and wind vectors (in m s^{-1}) on 305 K isentropic surface at 00Z February 28, 2001. Flight track of DC-8 mission 5 is indicated by the red line.

Plate 6. Along track cross-section of LIDAR O_3 (color shaded, in ppbv) and potential vorticity (contours, in 10^{-7} K m^2 kg^{-1} s^{-1}) for TRACE-P DC-8 flight 13 (Yokota local #1). Flight track is indicated by the red line.

Plate 7. Potential Vorticity (shaded, in 10^{-7} K m^2 kg^{-1} s^{-1}), pressure (green contours, in hPa), and wind vectors (in m s^{-1}) on 310 K isentropic surface at 18Z March 20, 2001. Flight track of DC-8 mission 13 is indicated by the red line.

Table 1. Properties of TRACE-P Layers, DC-8 and P-3 Aircraft, for H_2O, O_3, CO, CH_4

Type	Tracer	Obs	PC	Obs/km	h km	p hPa	ΔH km	Δp hpa	ΔH_2O %	ΔO_3 ppbv	ΔCO ppbv	ΔCH_4 ppbv
1A	$+O_3+H_2O+CO+CH_4$	22	7	0.02	5.5	531	0.59	41.4	24.4	18.7	58.9	23.1
1B	$+O_3+H_2O+CO-CH_4$	2	1	0.00	5.4	522	0.25	18.1	10.9	28.3	42.2	-16.0
1C	$+O_3+H_2O-CO+CH_4$	4	1	0.00	6.7	449	0.45	29.9	10.5	16.9	-18.6	12.0
1D	$+O_3+H_2O-CO-CH_4$	9	3	0.01	5.1	535	0.57	42.9	16.7	16.0	-16.8	-12.8
2A	$+O_3-H_2O+CO+CH_4$	74	23	0.06	4.9	560	0.58	41.3	-22.3	21.1	37.9	20.4
2B	$+O_3-H_2O+CO-CH_4$	15	5	0.01	5.7	512	0.66	41.6	-25.3	21.9	14.2	-13.2
2C	$+O_3-H_2O-CO+CH_4$	25	8	0.02	4.8	565	0.47	33.6	-15.0	22.1	-13.9	13.0
2D	$+O_3-H_2O-CO-CH_4$	69	22	0.06	5.4	521	0.59	39.3	-20.1	26.7	-21.1	-17.5
3A	$-O_3+H_2O+CO+CH_4$	16	5	0.01	5.3	537	0.36	23.3	34.0	-14.5	36.1	20.7
3B	$-O_3+H_2O+CO-CH_4$	5	2	0.00	4.5	592	0.26	19.1	21.0	-13.8	16.8	-7.4
3C	$-O_3+H_2O-CO+CH_4$	9	3	0.01	6.4	460	0.73	42.7	22.8	-14.9	-18.1	14.5
3D	$-O_3+H_2O-CO-CH_4$	20	6	0.02	4.5	583	0.53	37.4	20.7	-16.9	-31.0	-17.2
4A	$-O_3-H_2O+CO+CH_4$	9	3	0.01	5.7	504	0.38	24.0	-13.5	-17.9	15.6	11.4
4B	$-O_3-H_2O+CO-CH_4$	6	2	0.00	4.8	571	0.62	39.1	-10.3	-19.8	18.8	-10.8
4C	$-O_3-H_2O-CO+CH_4$	9	3	0.01	5.8	405	0.78	52.9	-22.2	-17.7	-18.2	14.5
4D	$-O_3-H_2O-CO-CH_4$	21	7	0.02	5.1	540	0.70	47.9	-19.2	-17.1	-44.1	-16.3
Average		315		0.25	5.2	538	0.57	38.8	21.0	20.8	29.2	17.2

Table 2. Occurrence and characteristics of atmospheric layers.
(a) Percentage of layer types for different missions.

	$-O_3/+H_2O$	$+O_3/-H_2O$	$-O_3/+H_2O$	$-O_3/-H_2O$
PEMA	14	54	15	18
PEMB	11	54	17	18
PEMTA	12	53	19	17
PEMTB	7	68	9	16
MOZAIC	15	50	17	18
TRACE-P	13	55	17	16

(b) Number, thickness, and height for layer types.

	$-O_3/+H_2O$			$+O_3/-H_2O$			$-O_3/+H_2O$			$-O_3/-H_2O$		
	No.	Th.*	Ht.*	No.	Th.	Ht.	No.	Th.	Ht.	No.	Th.	Ht.
PEMA	11	0.68	5.7	43	0.76	5.2	12	0.87	5.1	14	0.86	6.5
PEMB	8	0.59	6.5	38	0.99	6.0	12	0.64	6.0	13	0.49	6.4
PEMTA	27	0.45	6.0	120	0.71	5.2	43	0.47	5.4	38	0.45	6.1
PEMTB	14	0.40	6.6	133	0.49	5.6	18	0.92	7.6	31	0.57	7.2
MOZAIC	3,341	0.67	6.3	11,288	0.86	5.7	3,751	0.78	5.8	4,000	0.74	5.9
TRACE-P	60	0.46	4.9	254	0.58	5.3	79	0.56	5.2	73	0.59	5.8

* Thickness(Th.) and hight (Ht.) in km.

(c) Percentage of atmosphere occupied by layers.

	Profiles (km)	Ave. Thickness (km)	Total no. of layers	% Occupied
PEMA	439	0.78	80	14
PEMB	388	0.79	71	14
PEMTA	655	0.59	228	20
PEMTB	1330	0.54	196	8
MOZAIC	105,498	0.79	22,380	17
TRACE-P	1254	0.56	466	21

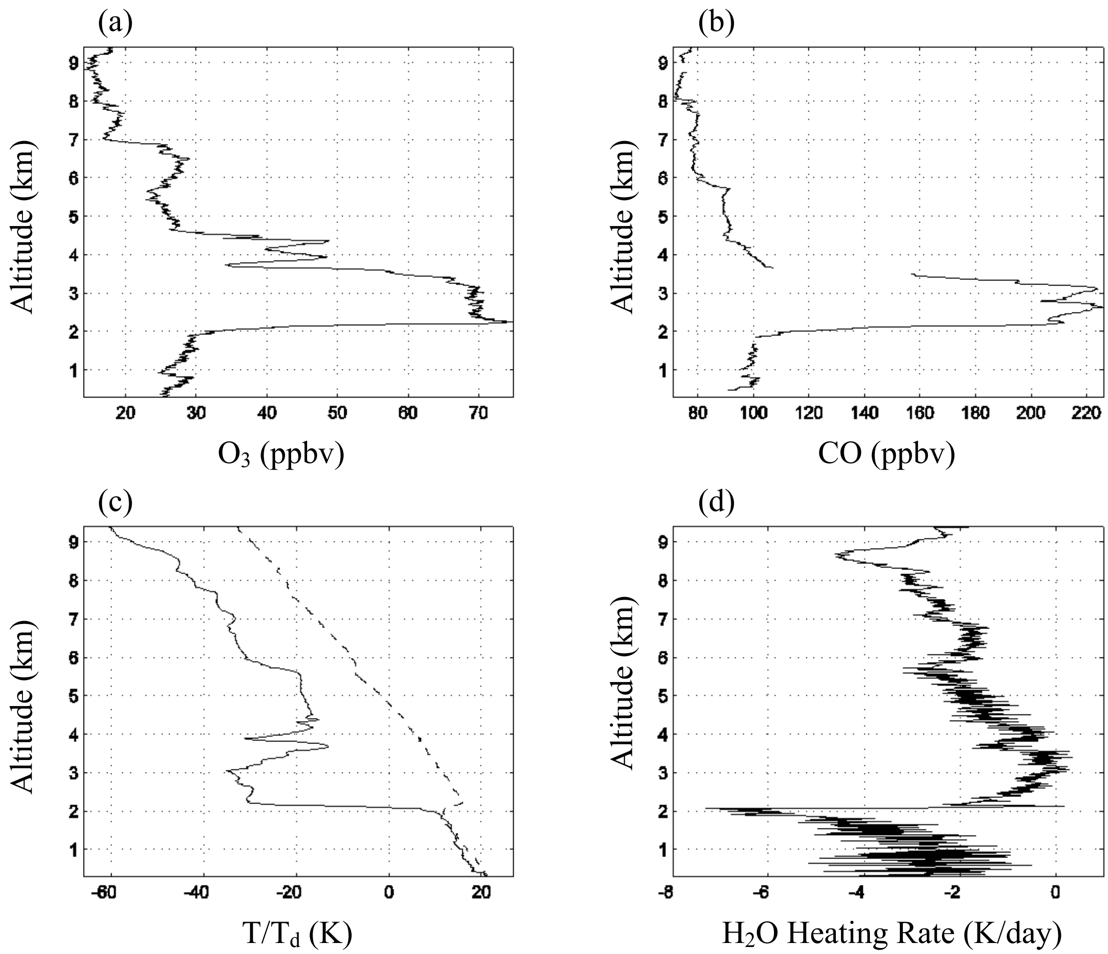

Figure 1. Vertical profiles of O_3, CO, air/dew-point temperatures, and H_2O heating rate sampled during TRACE-P DC-8 mission 5 around 22:40 UTC, February 27, 2001, near 18ºN, 175ºW.

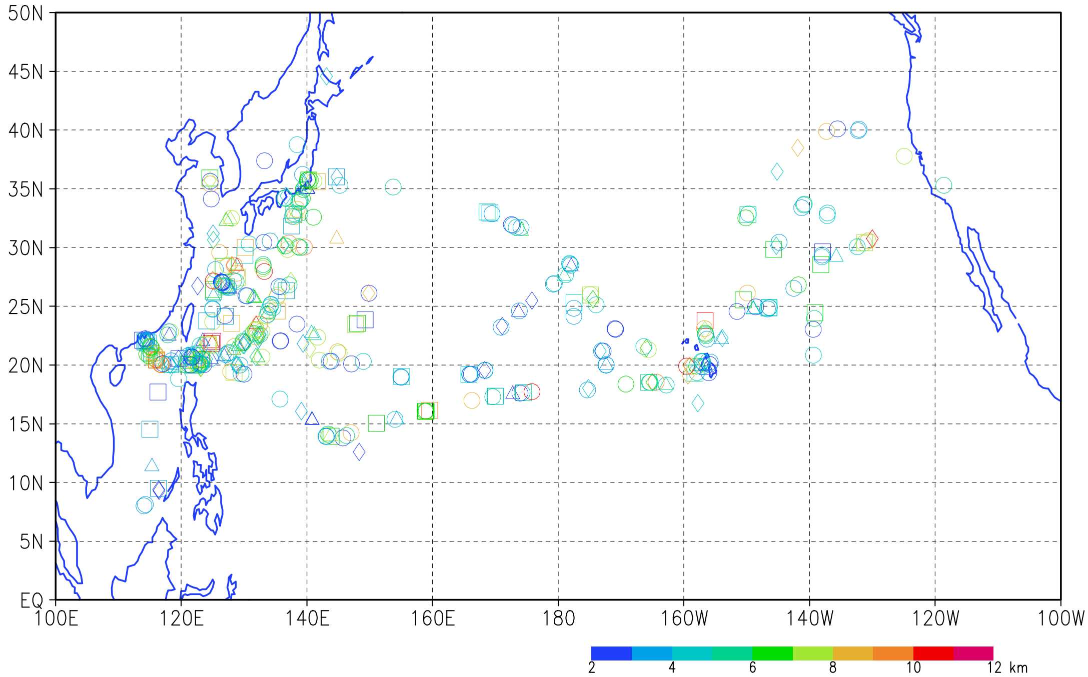

Plate 1. Geographical distribution of layers based on ozone and water vapor. Symbols indicate layers with rich O_3 and H_2O (triangles); rich O_3 and poor H_2O (circles); poor O_3 and rich H_2O (diamonds); poor O_3 and H_2O (squares). Layers are colored according to their altitudes fallen into 1 km bins shown in the color bar.

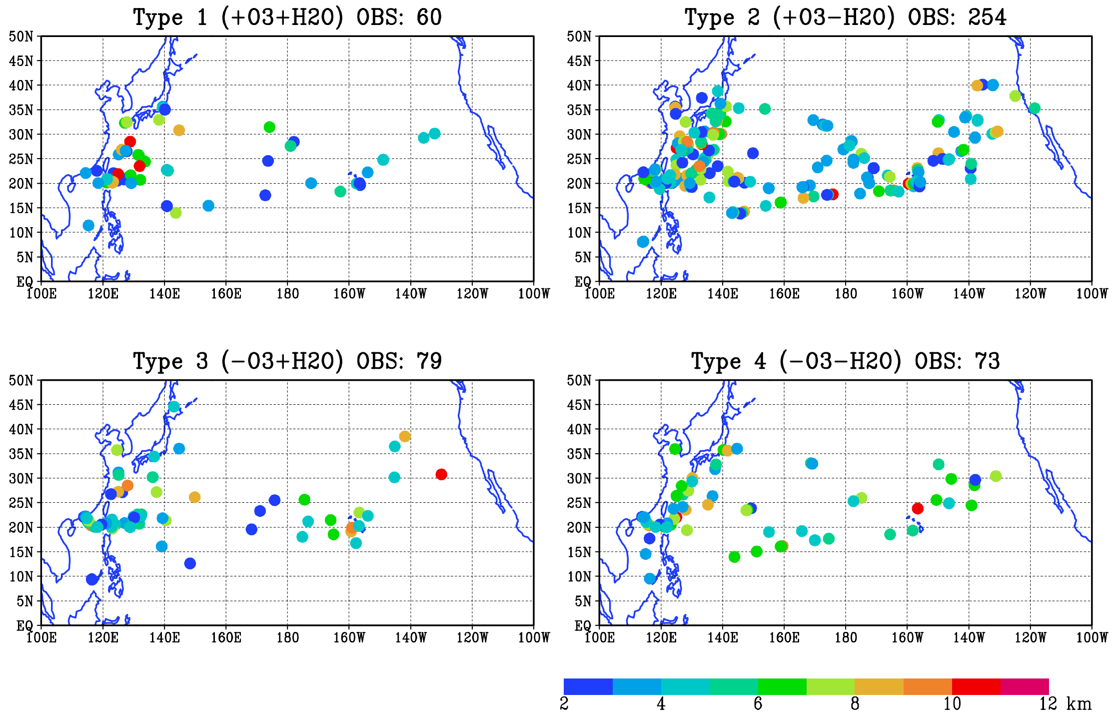

Plate 2. Same as Figure 1 with each category (based O_3 and H_2O only) displayed separately. Number of observations is indicated on each panel.

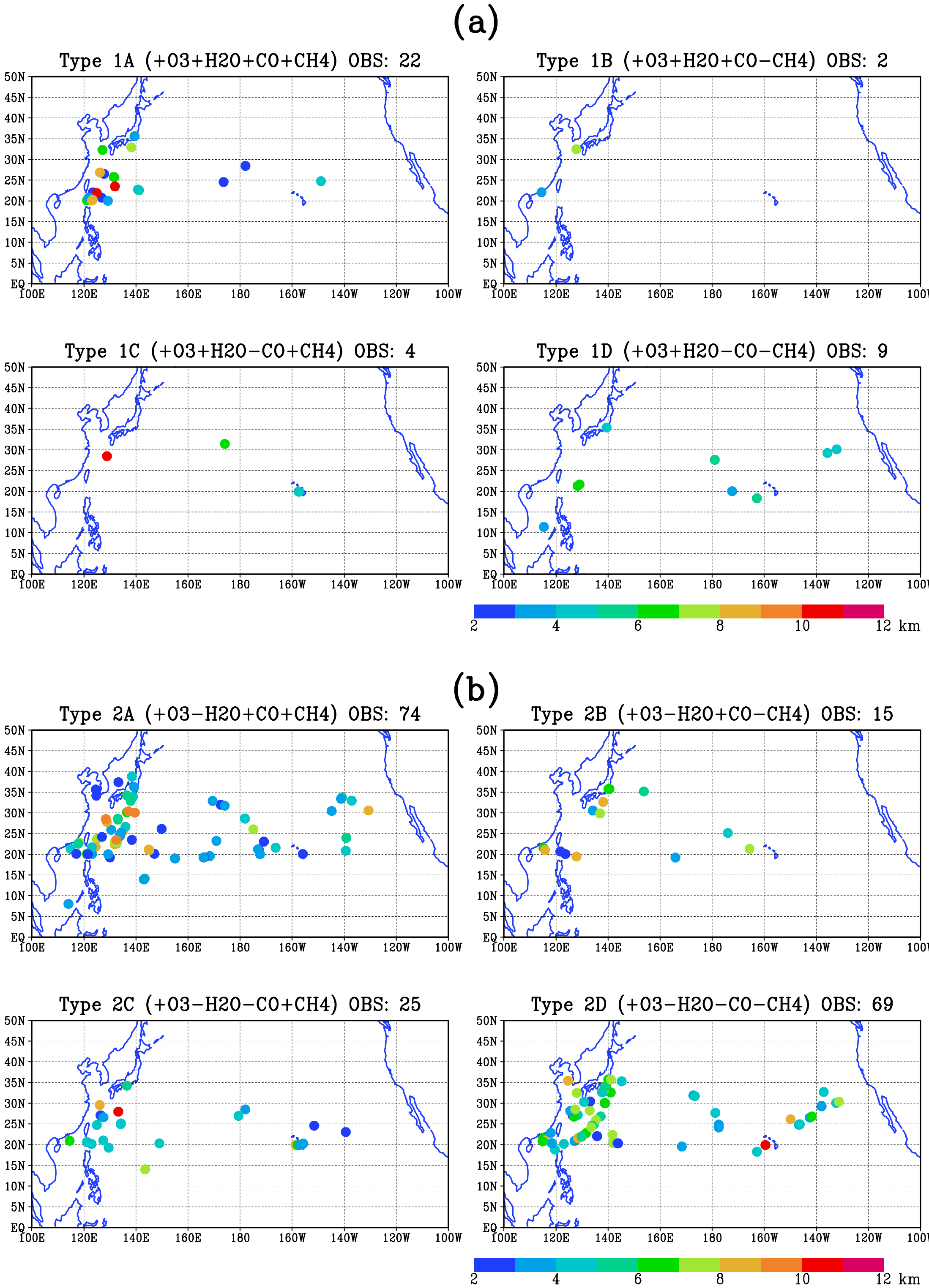

Plate 3. Geographical distribution of layers based on O_3, H_2O, CO, and CH_4 for (a) Type 1; (b) Type 2; (c) Type 3; (d) Type 4. Number of observations is indicated on each panel.

(c)

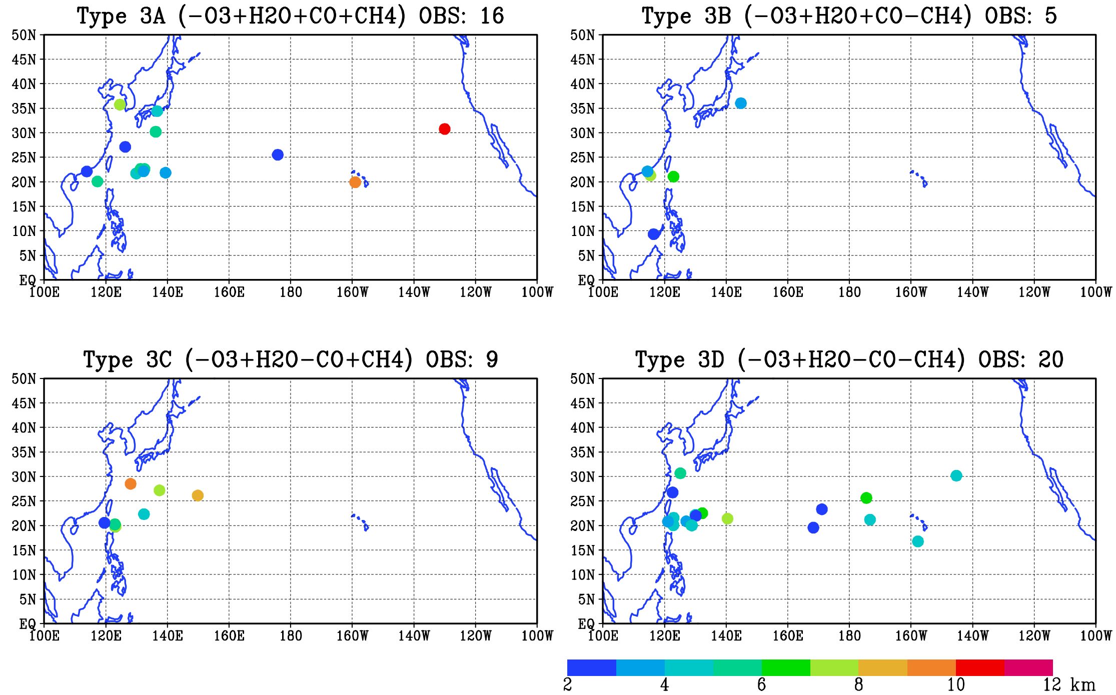

(d)

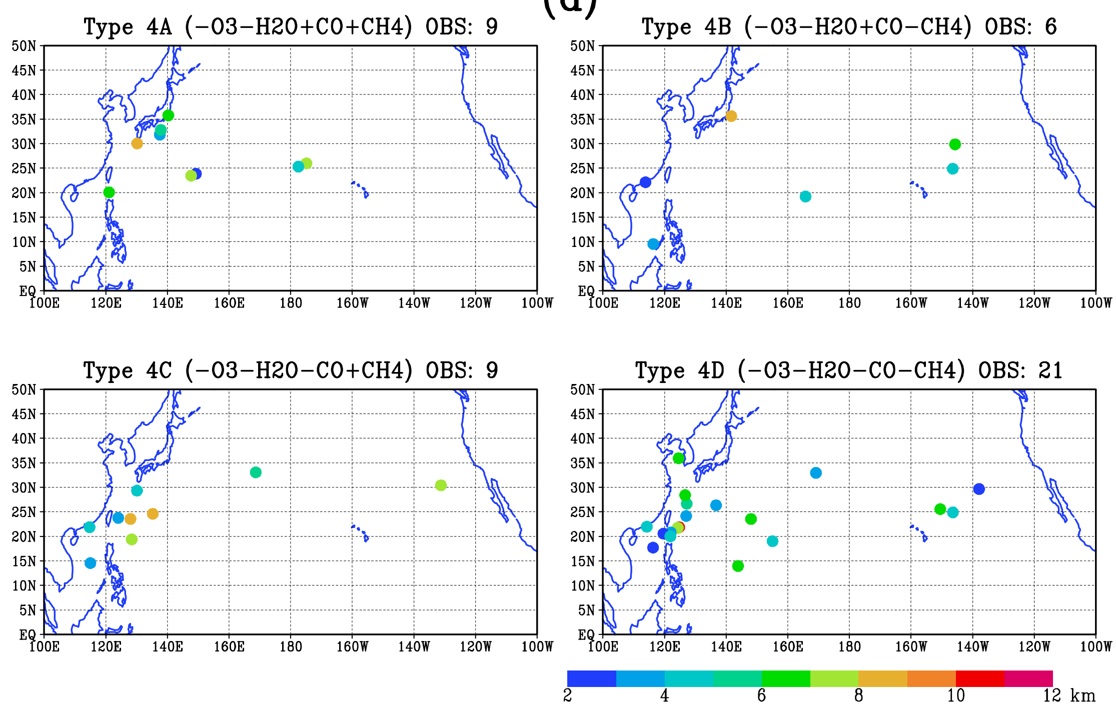

Plate 3. (*Continued*)

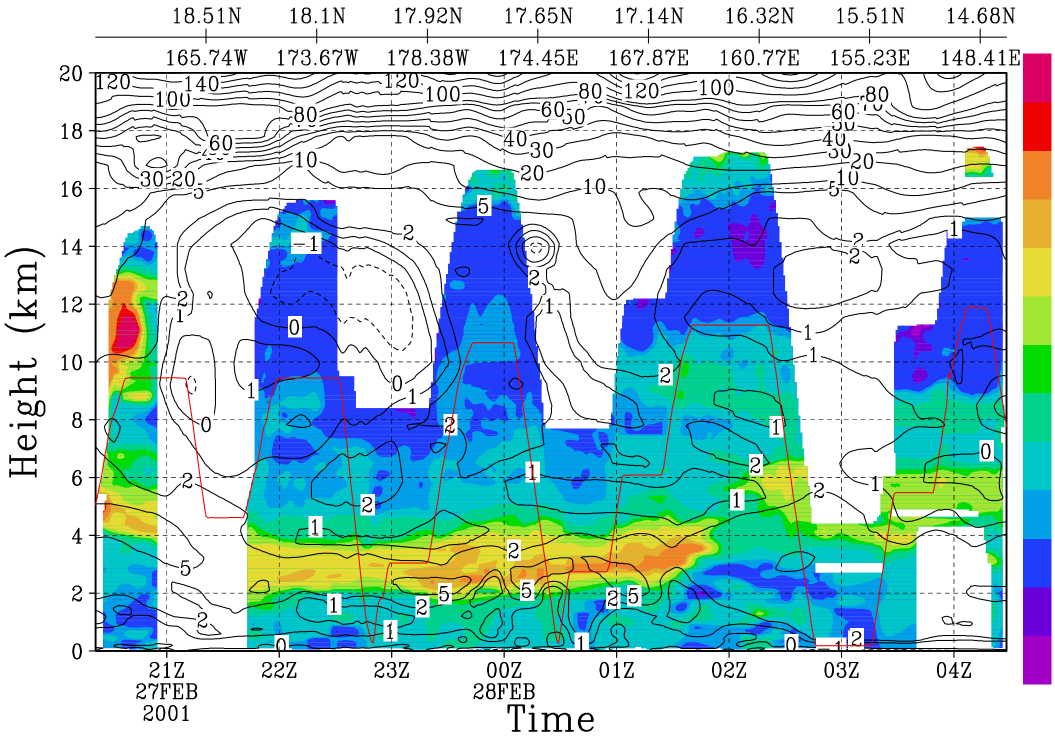

Plate 4. Along track cross-section of LIDAR O_3 (color shaded, in ppbv) and potential vorticity (contours, in 10^{-7} K m^2 kg^{-1} s^{-1}) for TRACE-P DC-8 flight 5 (Kona to Guam). Flight track is indicated by the red line.

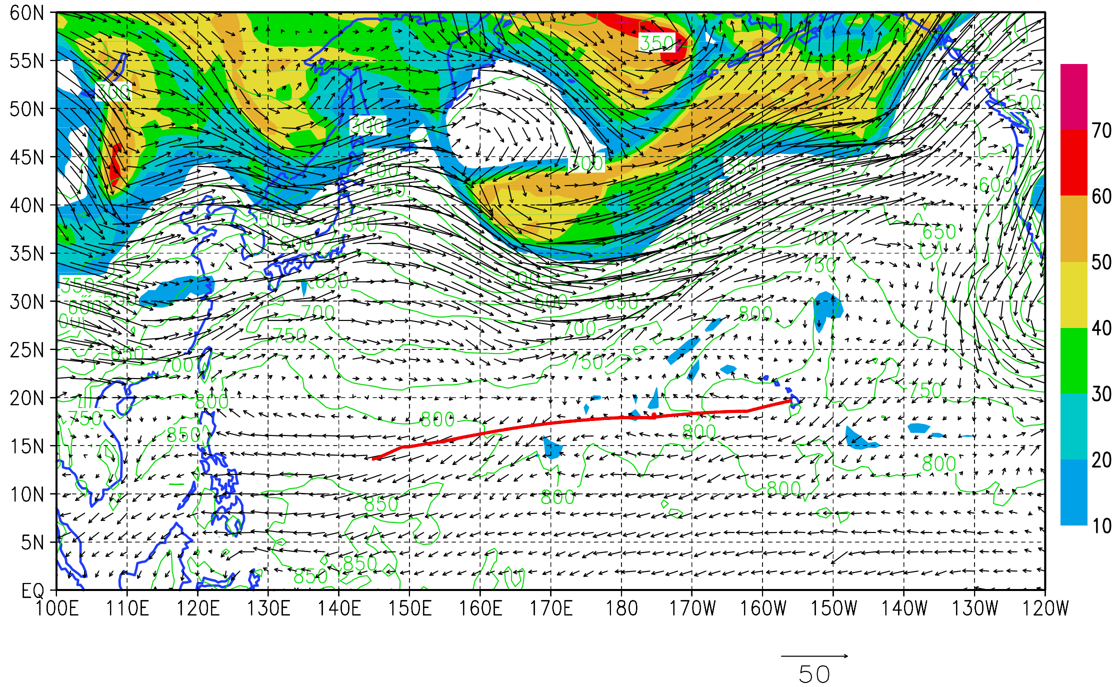

Plate 5. Potential Vorticity (shaded, in 10^{-7} K m^2 kg^{-1} s^{-1}), pressure (green contours, in hPa), and wind vectors (in m s^{-1}) on 305 K isentropic surface at 00Z February 28, 2001. Flight track of DC-8 mission 5 is indicated by the red line.

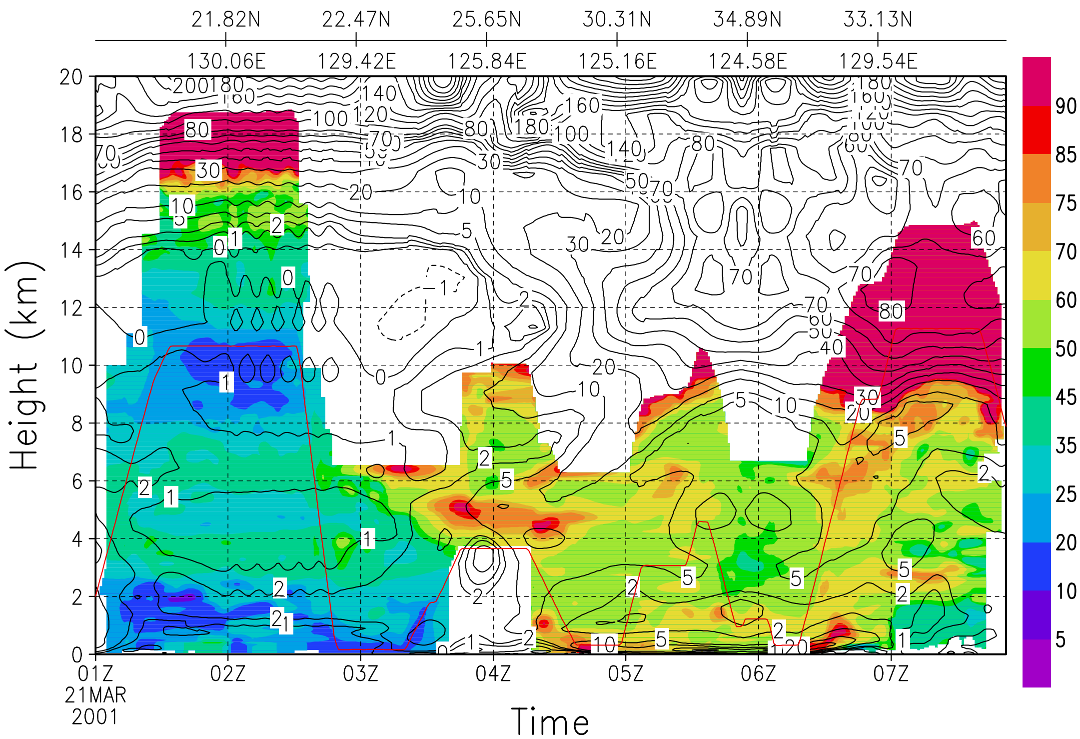

Plate 6. Along track cross-section of LIDAR O_3 (color shaded, in ppbv) and potential vorticity (contours, in 10^{-7} K m^2 kg^{-1} s^{-1}) for TRACE-P DC-8 flight 13 (Yokota local #1). Flight track is indicated by the red line.

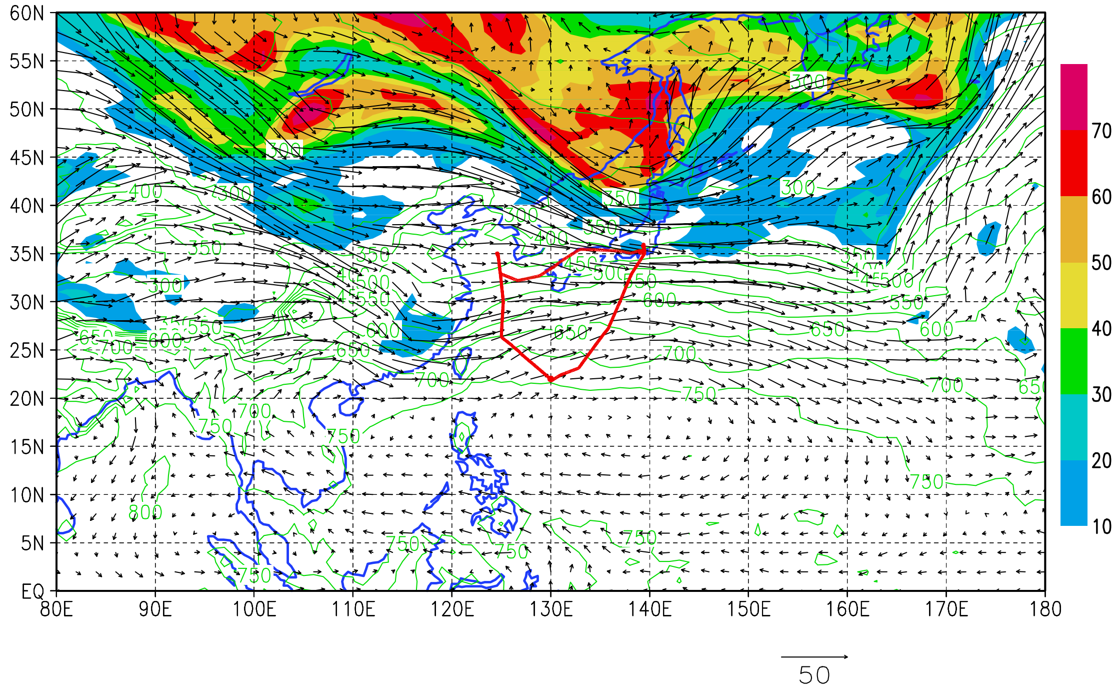

Plate 7. Potential Vorticity (shaded, in 10^{-7} K m^2 kg^{-1} s^{-1}), pressure (green contours, in hPa), and wind vectors (in m s^{-1}) on 310 K isentropic surface at 18Z March 20, 2001. Flight track of DC-8 mission 13 is indicated by the red line.